Methyl-β-cyclodextrin stimulates glucose uptake in Clone 9 cells: a possible role for lipid rafts

Kay BARNES*[1], Jean C. INGRAM*, Matthew D. M. BENNETT*, Gordon W. STEWART† and Stephen A. BALDWIN*

*School of Biochemistry and Molecular Biology, University of Leeds, Leeds LS2 9JT, U.K., and †Department of Medicine, University College of London, Rayne Institute, University Street, London WC1E 6JT, U.K.

An acute increase in the V_{max} for glucose uptake occurs in many mammalian cell types after exposure to osmotic or metabolic stress. In the rat epithelial Clone 9 cell line, the glucose transporter isoform GLUT1 is responsible for this enhanced uptake. Although stimulation of transport in these cells is known to result from the unmasking of 'cryptic' exofacial permeant-binding sites in GLUT1 molecules resident in the plasma membrane, the mechanism of such unmasking remains unclear. One possibility involves changes in the lipid environment of the transporter: reconstitution experiments have shown that transport activity *in vitro* is acutely sensitive to the phospholipid and cholesterol composition of the membrane. In the current study we found that treatment of Clone 9 cells with methyl-β-cyclodextrin, which removed > 80 % of the cell cholesterol, led to a 3.5-fold increase in the V_{max} for 3-*O*-methyl-D-glucose transport while having little effect on the K_m. In contrast to the metabolic stress induced by inhibition of oxidative phosphorylation, cholesterol depletion led neither to depletion of cellular ATP nor stimulation of AMP-activated protein kinase. Similarly, it did not result in stimulation of members of the stress- and mitogen-activated protein kinase families. In unstressed, cholesterol-replete cells, a substantial proportion of GLUT1 in detergent lysates co-fractionated with the lipid-raft proteins caveolin and stomatin on density-gradient centrifugation. Immunocytochemistry also revealed the presence of GLUT1-enriched domains, some of which co-localized with stomatin, in the plasma membrane. Both techniques revealed that the abundance of such putative GLUT1-containing domains was decreased not only by cholesterol depletion but also in cells subjected to metabolic stress. Taken together, these data suggest that a change in the lipid environment of GLUT1, possibly associated with its re-distribution between different microdomains of the plasma membrane, could play a role in its activation in response to stress.

Key words: cholesterol, GLUT1, stomatin, stress, transport.

INTRODUCTION

An acute increase in the V_{max} for glucose uptake with little or no change in the apparent affinity (K_m) for the permeant occurs in many mammalian cells after exposure to metabolic stresses such as hypoxia or inhibition of oxidative phosphorylation, or to osmotic stress [1,2]. In the rat epithelial Clone 9 cell line, the GLUT1 glucose transporter isoform is known to be responsible for such stress-induced increases in glucose uptake [3]. Interestingly, changes in the V_{max} for transport in these cells were found to occur in the absence of any change in the total number of cell-surface glucose transporters. Instead, transport stimulation was found to be associated with the unmasking of 'cryptic' exofacial permeant-binding sites in GLUT1 molecules already resident in the plasma membrane [3–5].

The mechanism of GLUT1-binding site unmasking in cells subjected to stresses remains unclear. However, several observations led us to hypothesize that stress-induced changes in the lipid environment of the transporters might be involved. For example, it has long been known from reconstitution experiments with the purified GLUT1 protein that its transport activity is very sensitive to the phospholipid and cholesterol composition of the bilayer [6]. While acute changes in membrane composition in stressed cells are unlikely, stress-induced redistribution of the transporter between membrane domains of differing lipid composition might therefore affect its activity. The plasma membranes of eukaryotic cells are well known to contain specialized microdomains or 'rafts' enriched in sphingolipids and cholesterol [7]. It is the biophysical properties of the sphingolipids and cholesterol that result in the partitioning of these tightly packed liquid-ordered domains, approx. 10 nm to 1 μm in size, away from the less-organized glycerophospholipids in the bulk of the membrane [8–10]. Characteristically, rafts may also be enriched in glycosylphosphatidylinositol-anchored proteins [11,12], in the caveolae marker protein, caveolin [13], and in signal transduction molecules (for review see [14]). The latter have recently been shown to include components of the insulin signalling cascade such as the Rho-family GTPase TC10 and the cbl–Cap complex. These proteins are essential for insulin-stimulated glucose uptake and translocation of the transporter isoform GLUT4 in adipocytes [15–18].

Recently, GLUT1 transporters were reported to be localized in part to detergent-resistant membrane domains in a number of cell types [19]. Moreover, evidence has been obtained supportive of a specific interaction between GLUT1 and the lipid-raft-associated protein stomatin [20]. In conjunction with the known sensitivity of the transporter to its lipid environment, we were therefore prompted to hypothesize that stress-induced re-distribution of the GLUT1 transporter between different sub-domains of the membrane, including cholesterol-rich lipid rafts, might play a role in its activation. To investigate this hypothesis, in the present study we investigated the effects of cholesterol depletion on hexose uptake in Clone 9 cells in the presence and absence of metabolic stress. In parallel, the effects of these treatments

Abbreviations used: AMPK, AMP-activated protein kinase; JNK, c-Jun N-terminal kinase; KRH, Krebs–Ringer Hepes buffer; KRHG, Krebs–Ringer Hepes containing 25 mM glucose; MβCD, methyl-β-cyclodextrin; p38 MAPK, p38 mitogen-activated protein kinase.

[1] To whom correspondence should be addressed (e-mail k.barnes@leeds.ac.uk).

on the association of GLUT1 with lipid rafts was probed both by immunocytochemical studies of transporter distribution in the plasma membrane and by density-gradient centrifugation of detergent-treated cell lysates. Taken together the resultant data suggest that a change in the lipid environment of GLUT1, possibly associated with its re-distribution between different microdomains of the plasma membrane, may play a role in the activation of the transporter in response to stress.

MATERIALS AND METHODS

Expression and purification of a C-terminal fragment of stomatin

A full-length cDNA clone (CloneID 1122198) encoding mouse stomatin was obtained from the I.M.A.G.E. Consortium [21] via the MRC Human Genome Mapping Project Resource Centre. The sequence encoding the large, hydrophilic, cytoplasmic domain in the C-terminal region of the protein (residues 92–286) was amplified from the clone using *Pfu* polymerase and the forward and reverse primers 5′-CGAGGATCCAAGGTGGACATGAGGACCATC-3′ and 5′-GTCAAGCTTTCAGTGATTAGAACCCATGATGCC-3′ respectively. The PCR product was subcloned into the bacterial expression vector pET-28a(+) (Novagen) using *Bam*HI and *Hin*dIII restriction sites (underlined above) incorporated into the 5′ ends of the primers. The resultant construct encoded the C-terminal two-thirds of the stomatin protein with an N-terminal hexahistidine tag for purification purposes. Following expression in *Escherichia coli* BL21(DE3)pLacI (Novagen), the His_6-tagged stomatin C-terminal fragment was purified to homogeneity by metal-chelate affinity chromatography on a column of Ni-NTA (Ni^{2+}-nitrilotriacetic acid)–agarose (Qiagen, Crawley, West Sussex, U.K.). Antibodies were raised in sheep against the purified protein, and affinity-purified by chromatography on a column of stomatin C-terminal fragment immobilized on CNBr-activated Sepharose 4B (Sigma-Aldrich, Poole, Dorset, U.K.).

Cell culture and sugar-transport assays

Clone 9 cells were cultured in six-well plates or in 75 cm^2 dishes as described previously [22]. Cells were grown to confluence and initial rates of radiolabelled sugar uptake were estimated using a modification of a previously described protocol [3,22]. For 3-*O*-methyl-D-glucose transport measurements, uptake was initiated by addition to each well of 0.5 ml of 0.1 mM 3-*O*-[methyl-^{3}H]D-glucose in KRH (Krebs–Ringer Hepes buffer; 136 mM NaCl, 20 mM Hepes, 4.7 mM KCl, 1.25 mM $MgSO_4$ and 1.25 mM $CaCl_2$, pH 7.4) at 22 °C, and the uptake was measured for a period of 1.5 min. Transport was stopped using three washes in 50 μM phloretin in ice-cold PBS (150 mM NaCl and 12.5 mM NaH_2PO_4, pH 7.4). Cells were lysed with 0.5 ml of 1 % Triton X-100, and radioactivity measured by liquid-scintillation counting. Transporter-mediated uptake rates were calculated by subtracting non-specific uptake measured in the presence of 20 μM cytochalasin B. Uptake of [^{3}H]2-deoxy-D-glucose was measured in a similar fashion, except that a permeant concentration of 0.2 mM was employed and the uptake period was 5 min at 37 °C. Pre-incubations of cells with appropriate concentrations of stress-inducing (i.e. sodium azide) or cholesterol-depleting [i.e. MβCD (methyl-β-cyclodextrin)] agents in KRHG (KRH plus 25 mM glucose) were carried out for 15–60 min at 37 °C prior to measurement of glucose uptake, as indicated in the Figure legends. Data are presented as means ± S.E.M. (n, except where stated, is the number of experiments carried out). Significance was assessed using a Student's t test for two groups and was taken as $P < 0.05$. For measurements of relative cholesterol contents, cells were pre-incubated at 37 °C for 16 h with [^{3}H]cholesterol (0.5 μCi/ml) in cell culture medium [23]. After treatment with or without MβCD cells were washed in PBS, lysed at 22 °C with 1 % Triton X-100 in PBS, and then radioactivity present in the lysates was quantified by liquid-scintillation counting.

Preparation of lipid rafts

Lipid rafts and detergent-soluble proteins were separated by flotation assays adapted from previously described methods [24,25]. Confluent Clone 9 cells in 10 cm-diameter dishes (approx. 1 mg of protein per dish) were washed twice with 10 ml of KRH/EDTA (KRH containing 5 mM EDTA). To each dish 2 ml of KRH/EDTA was then added and the cells were scraped into a 15 ml Falcon tube (for each treatment the cells from four dishes were pooled). The cells were pelleted at 1000 ***g*** for 5 min and then left on ice for 10 min. The cell pellet was incubated at 4 °C in 0.5 ml of 0.5 % Triton X-100 in KRH/EDTA supplemented with a cocktail of protease inhibitors for use with mammalian cell and tissue extracts (Sigma-Aldrich). In all subsequent steps, solutions and samples were kept at 4 °C. Cells were next homogenized by passage through a 21 guage needle. For Nycodenz gradient separations, 500 μl of 70 % Nycodenz prepared in KRH/EDTA was mixed with an equal volume of homogenized sample and then overlaid with an 8–35 % Nycodenz linear step gradient (400 μl each of 25, 22.5, 20, 18, 15, 12 and 8 % Nycodenz in KRH/EDTA). After centrifugation in an SW55 Beckman rotor at 200 000 ***g*** for 18 h at 4 °C, twelve 340 μl fractions were collected from the gradient.

For sucrose-gradient separations, 500 μl of the cell homogenate was first centrifuged at low speed (800 ***g***, 10 min) to remove unbroken cells and nuclear debris. The resultant supernatant was aspirated, mixed with an equal volume of 80 % sucrose and loaded under a sucrose gradient (2 ml each of 5 % and 35 % sucrose in KRH/EDTA). The gradient was then centrifuged at 150 000 ***g*** as described above. Ten 500 μl samples were collected from each gradient. Ice-cold methanol (1 ml) was added to each of the samples collected from either the Nycodenz or sucrose gradients. The samples were then subjected to centrifugation for 30 min at 13 000 ***g*** and the resultant protein precipitates were dissolved in 50 μl of SDS sample buffer.

Western blotting and immunocytochemistry

For Western blotting, proteins were subjected to electrophoresis on SDS/10 % (w/v) polyacrylamide gels and then transferred to nitrocellulose membranes. Blots were probed overnight at 4 °C with affinity-purified rabbit antibodies (0.5 μg/ml) against residues 477–492 of rat GLUT1 [26] or caveolin (Transduction Laboratories, Lexington, KY, U.S.A.), or with a rabbit antiserum raised against a glutathione S-transferase fusion protein bearing the C-terminal region of human stomatin (residues 141–288) [27]. Affinity-purified rabbit antibodies against the phosphorylated forms of AMPK-α (AMP-activated protein kinase-α) and p38 MAPK (p38 mitogen-activated protein kinase) were purchased from Cell Signalling Technology™, New England Biolabs, Hitchen, Herts., U.K. Blots were also stained with mouse monoclonal antibodies against tubulin (Sigma-Aldrich), against the human transferrin receptor (Zymed Laboratories, Cambridge BioScience, Cambridge, U.K.) and against p46 and p54 JNK (c-Jun N-terminal kinase) dually phosphorylated at Thr-183

and Tyr-185 (Cell Signalling Technology™). Secondary antibodies, horseradish peroxidase conjugates of goat anti-rabbit or anti-mouse IgG (diluted 1/50 000; Jackson ImmunoResearch Laboratories, Stratech Scientific, Soham, Cambs., U.K.), were applied as appropriate for 1 h. The antigens were then visualized by addition of enhanced chemiluminescence detection reagents (Supersignal® chemiluminescent substrate, Pierce Chemical Company, Tattenhall, Cheshire, U.K.). Staining intensity was quantified using a Bio-Rad Fluor-S gel documentation system and Multi-analyst software.

Plasma membrane lawns were prepared as described previously [2,26]. They were stained for rat GLUT1 using affinity-purified rabbit antibodies (20 μg/ml) raised against synthetic peptides corresponding to the C-terminal region of the protein (residues 477–492) or to a portion of the central cytoplasmic loop (residues 231–246), followed by biotinylated donkey anti-rabbit IgG and streptavidin-FITC. Where stated in the Figure legends, the C-terminus of stomatin (residues 92–284; 0.023 μg/μl) in Hepes buffer (150 mM NaCl and 50 mM Hepes, pH 7.4) was applied to unfixed plasma membrane lawns for 16 h at 4 °C prior to fixing and immunostaining. Images were obtained and quantified (except where indicated in the Figure legends) with a Nikon microscope linked to a CCD camera and Openlab deconvolution software (Improvision, Warwick, U.K.). Quantification data for GLUT1-enriched domains were obtained with the Openlab software from three independent experiments.

For dual-labelling immunofluorescence studies, affinity-purified rabbit antibodies (20 μg/ml) against a synthetic peptide corresponding to residues 231–246 in the central cytoplasmic loop of rat GLUT1 and affinity-purified sheep antibodies (20 μg/ml) against the C-terminal region of stomatin (residues 92–284) were applied simultaneously. The bound antibodies were then respectively detected by staining with a Texas Red conjugate of donkey anti-rabbit IgG and with biotinylated donkey anti-sheep IgG (Jackson ImmunoResearch Laboratories) followed by Streptavidin Alexa Fluor488 (Molecular Probes, Leiden, The Netherlands). For imaging, 20 optical sections were captured at 0.2 μm intervals with a Delta Vision® system (Applied Precision, Issaquah, WA, U.S.A.) comprising an Olympus IX70 microscope linked to a CCD camera, and processed using the manufacturer's deconvolution software.

ATP assay

ATP was measured by using a Bioluminescence Assay Kit HSII (Roche, Basel, Switzerland.). Confluent Clone 9 cells grown in 75 cm^2 dishes were treated (two dishes per treatment) with 5 mM sodium azide or 10 mM MβCD in KRHG or with KRHG only for periods of 15 and 30 min. The cells were washed once in 10 ml of PBS (Gibco). They were then scraped from the dish in 1 ml of PBS into a 15 ml Falcon tube and centrifuged for 3 min at 1000 ***g***. After adding 60 μl of the kit cell lysis buffer to the cells that had been heated to 90 °C, the resultant lysate was transferred to a 1.5 ml tube and left for 2 min on a heating block at 90 °C. The lysate was subjected to centrifugation for 60 s at 13 000 ***g*** and the supernatant was transferred to a fresh tube and kept on ice. The ATP standard curve and samples were set up according to the manufacturer's instructions and the changes in luminescence were measured using a Mediators PhL luminometer and associated software.

Protein assay

Protein concentrations were determined by the bicinchoninic acid method with BSA as standard [28].

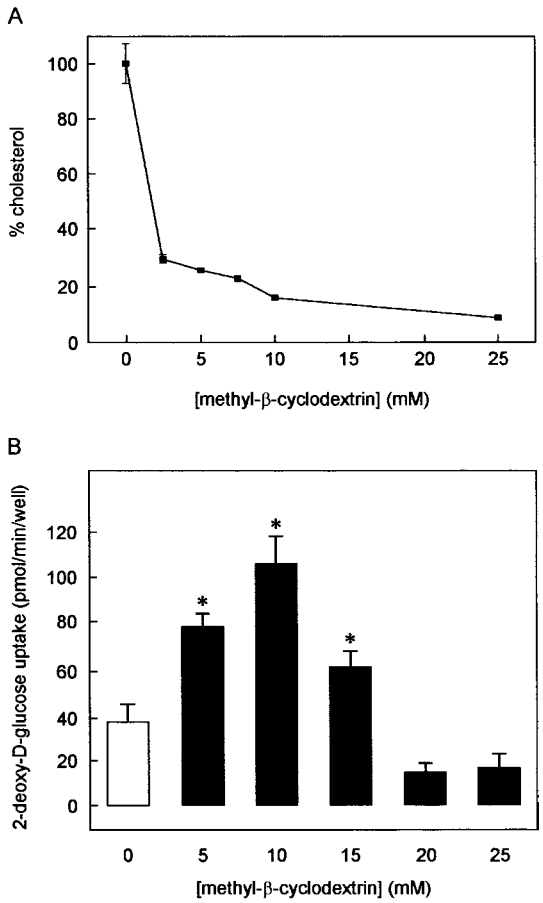

Figure 1 Effects of MβCD on cell membrane cholesterol content and hexose uptake

(**A**) To quantify the removal of cholesterol from the cell membranes, Clone 9 cells were incubated with [^{3}H]cholesterol (0.5 μCi/ml) in cell culture medium for 16 h at 37 °C, prior to treatment with MβCD for 60 min at the concentrations indicated. Cells were washed with PBS at 37 °C, lysed with 1 % Triton X-100 in PBS at 4 °C and the [^{3}H]cholesterol content was estimated by liquid-scintillation counting. (**B**) Confluent cells were pre-incubated with 5, 10, 15, 20 or 25 mM MβCD for 60 min or left untreated prior to measurement of the uptake of 0.2 mM [^{3}H]2-deoxy-D-glucose. Results in (**A**) and (**B**) are expressed as mean $\pm$ S.E.M. ($n = 3$). *Significantly different ($P < 0.05$) from the control (untreated cells).

RESULTS

Effect of cholesterol-depletion on glucose uptake in Clone 9 cells

In *in vitro*-reconstituted systems, GLUT1 activity and hence glucose uptake has been shown to be modulated by its lipid environment, in particular by the cholesterol content of the membrane [29]. To assess the possible role of cholesterol in regulating transport activity *in vivo*, we treated Clone 9 cells for 60 min with the cholesterol-depleting agent MβCD [30], at the concentrations indicated in Figure 1. Measurements of [^{3}H]cholesterol levels in cells that had been pre-equilibrated with this lipid showed that treatment with 10 mM MβCD for 60 min removed > 80 % of the cell cholesterol (Figure 1A). Treatment of Clone 9 cells with MβCD up to a concentration of 10 mM caused a dose-dependent stimulation of hexose uptake. At higher concentrations of the cholesterol-depleting reagent, the stimulatory effect on transport decreased: at concentrations of 20 and 25 mM MβCD hexose uptake fell to < 50 % basal levels, possibly reflecting a toxic effect of the compound (Figure 1B). The effect of 10 mM MβCD was also time-dependent,

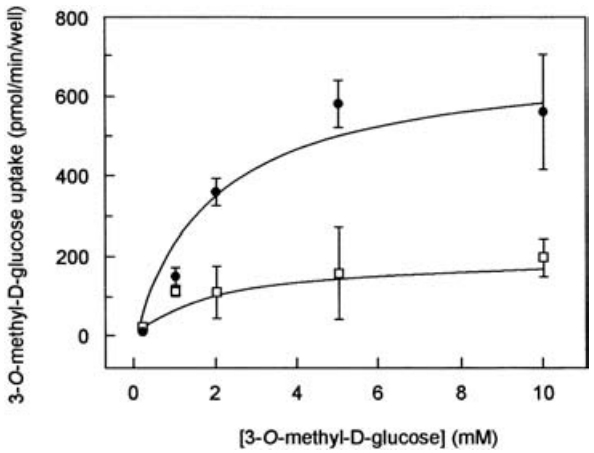

Figure 2 Effect of cholesterol depletion on the kinetic parameters of hexose uptake

Clone 9 cells were treated for 60 min with (●) or without (□) 10 mM MβCD. Uptake of [^{3}H]3-*O*-methyl-D-glucose was then measured at 22 °C in the presence of increasing concentrations of hexose as described in the Materials and methods section. Data shown are the means ± S.E.M. ($n = 3$). Transport parameters were estimated from the data by non-linear curve fitting to the Michaelis–Menten equation using Origin version 7 (OriginLab Corporation).

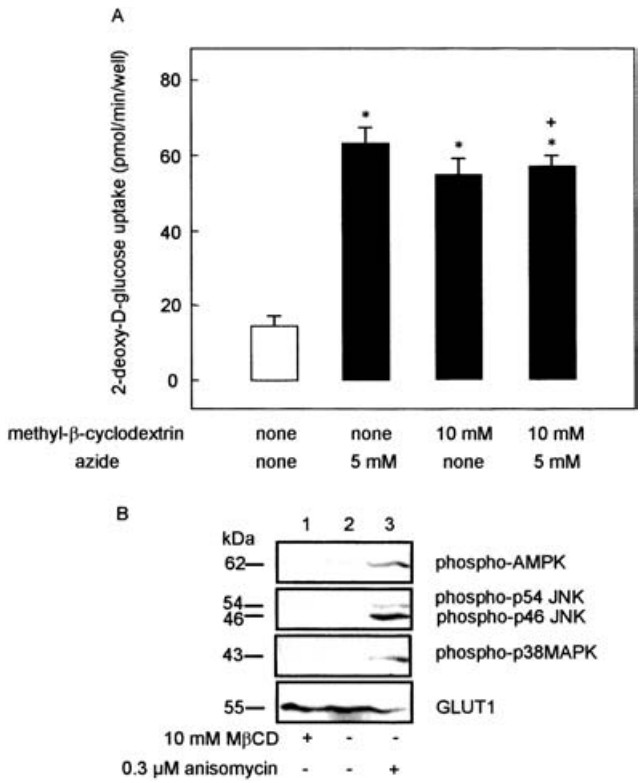

Figure 3 Effects of cholesterol depletion and metabolic stress on hexose uptake and phosphorylation of stress kinases

(**A**) Confluent Clone 9 cells were incubated with or without 10 mM MβCD for 60 min and then treated for a further 30 min with or without 5 mM sodium azide for 30 min, before measurement of the rate of uptake of 0.2 mM [^{3}H]2-deoxy-D-glucose. Results are expressed as mean ± S.E.M. ($n = 3$). *Significantly different ($P < 0.05$) from control (untreated cells); $^+$not significantly different ($P > 0.05$) from cells treated either with MβCD or azide alone. (**B**) Confluent Clone 9 cells were incubated with 10 mM MβCD for 60 min or 0.3 μM anisomycin for 45 min or left untreated before washing in KRH/EDTA buffer containing 5 mM EGTA, 50 mM NaF, 5 mM $Na_4P_2O_7$ and 5 mM Na_2VO_3, as described in the Materials and methods section. They were then lysed with 2 % SDS sample buffer and 30 μl samples of lysate proteins were analysed by electrophoresis and Western blotting. Blots were probed with antibodies to the phosphoproteins indicated and also to GLUT1.

reaching a maximum at 60 min (results not shown). Therefore, in subsequent experiments the maximum MβCD concentration used was 10 mM and the exposure period was limited to 60 min. An investigation into the kinetics of hexose uptake by cholesterol-depleted cells showed that, like the effects of inhibition of oxidative phosphorylation by azide [4,22], exposure to hypertonic conditions [2] or treatment with AICAR (5-aminoimidazole-4-carboxamide ribonucleoside) [3], MβCD treatment increased the V_{max} for transport with little effect on K_m. Exposure to 10 mM MβCD for 60 min increased the V_{max} for 2-deoxy-D-glucose uptake from 114 ± 19 ($n = 3$) to 173 ± 21 pmol/min/well ($n = 3$), whereas the K_m values of 0.55 ± 0.1 ($n = 3$) and 0.59 ± 0.1 mM ($n = 3$) measured in the control and MβCD-treated cells, respectively, were not significantly different. Because 2-deoxy-D-glucose is toxic to cells at high concentrations, the V_{max} and K_m were also measured using 3-*O*-methyl-D-glucose as the permeant (Figure 2). The V_{max} for uptake of this non-metabolizable glucose analogue was increased from 232 ± 90 pmol/min/well ($n = 3$) in control cells to 815 ± 125 pmol/min/well ($n = 3$) following treatment with MβCD, while the K_m values, at 2.1 ± 0.2 ($n = 3$) and 3.1 ± 1 mM ($n = 3$) respectively, were not significantly different. The saturable nature of hexose uptake into MβCD-treated cells, and its sensitivity to inhibition by cytochalasin B, showed that transport stimulation stemmed from an effect on the GLUT1 transporter rather than from a non-specific increase in membrane permeability induced by cholesterol depletion.

Effect of MβCD on stimulation of hexose uptake by metabolic stress, and on cellular ATP levels

Stimulation of hexose uptake by treatment of cells with MβCD resembled that previously reported for cells subjected to metabolic stress as a result of treatment with sodium azide [1,2]. To assess the possibility that the mechanisms of transport stimulation were similar in the two cases, the effects of exposing cells singly or simultaneously to stress and to cholesterol depletion were compared. 2-Deoxy-D-glucose uptake was stimulated 4.3 ± 0.13 ($n = 3$)-fold in cells subjected to metabolic stress by exposure for 30 min to 5 mM sodium azide in the absence of cholesterol depletion (Figure 3). Cholesterol depletion of an identical batch of cells by treatment with 10 mM MβCD for 60 min led to a similar 3.8 ± 0.29 ($n = 3$)-fold increase in glucose transport (Figure 3). Interestingly, no significant differences in hexose uptake levels were found between cells that had been treated for 30 min with 5 mM sodium azide, and cells that were subjected to this treatment following cholesterol depletion by exposure to 10 mM MβCD for 60 min (Figure 3). The lack of additivity of the effects of cholesterol depletion and of metabolic stress suggested that the mechanism of transport stimulation might be the same for the two stimuli.

Inhibition of oxidative phosphorylation by cyanide or azide is known to cause acute and extensive depletion of ATP in many cell types. For example, a 90 % decrease in cellular ATP levels within 20 min has been reported for Clone 9 cells subjected to such stresses [1,31]. A possible explanation for the effect of cyclodextrin was that treatment with this agent induced a similar decrease in cellular ATP levels. To examine this possibility ATP levels were measured in azide- and cyclodextrin-treated Clone 9 cells. As expected, treatment with 5 mM sodium azide led to ATP depletion: after 15 min exposure to the inhibitor, ATP levels were decreased 0.5 ± 0.03 ($n = 3$)-fold relative to untreated cells.

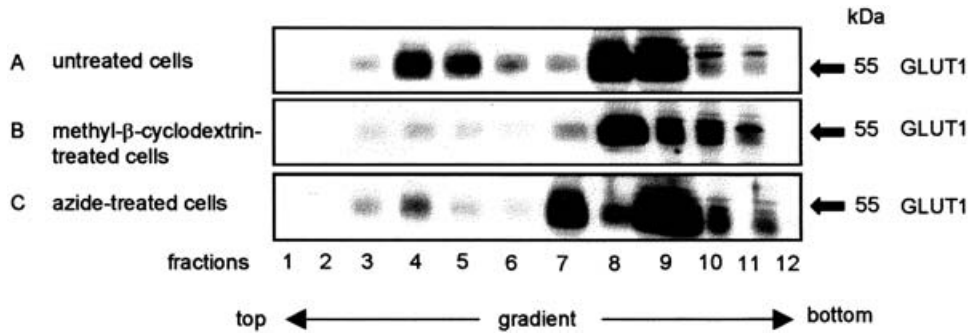

Figure 4 Effects of cholesterol depletion and metabolic stress on the plasma membrane distribution of GLUT1 in Clone 9 cells

Confluent Clone 9 cells were left untreated (**A**) or treated with 10 mM MβCD for 60 min (**B**) or 5 mM sodium azide for 30 min (**C**), as described in the Materials and methods section. The cells were washed in KRH/EDTA, scraped into a Falcon tube, precipitated by centrifugation and solubilized in 0.5 ml of 0.5 % Triton X-100 in KRH/EDTA buffer at 4 °C. The resultant lysates were separated by ultracentrifugation on a Nycodenz step gradient. To detect GLUT1 a 25 μl sample of the proteins from each fraction was subjected to Western blotting as described in the Materials and methods section.

However, cholesterol depletion did not result in a similar loss of ATP: ATP levels increased 1.5 ± 0.02 ($n = 3$)-fold following exposure of cells to 10 mM MβCD for 15 min, and after 30 min had returned to the values seen in untreated cells. These data suggested that, while the mechanisms of transport stimulation following exposure to metabolic stress or cholesterol depletion might have features in common, MβCD did not signal via ATP depletion.

Regulation of glucose transport in response to stresses has been reported to involve a variety of stress-activated kinases [2,3,22]. To examine the possibility that the effects of cholesterol depletion on transport were similarly mediated by such kinases, rather than by changes in the lipid environment of the transporter, phospho-specific antibodies were used to assess the effects of cholesterol depletion on the activation state of these proteins. Western blotting using these antibodies showed that the phosphorylated, activated forms of AMPK, p38 MAPK and JNK were undetectable in Clone 9 cells either before or after cholesterol depletion by treatment with MβCD (Figure 3B). In contrast, the phosphorylated forms of all three proteins were readily detectable in extracts of cells incubated for 45 min with 0.3 μM anisomycin, a potent activator of stress kinases [32]. Equal loading of samples from control, cholesterol-depleted and anisomycin-treated cells was confirmed by densitometry of the blots following staining for GLUT1. These data suggested that the stress kinases are unlikely to be involved in increased hexose uptake resulting from cholesterol depletion.

Effects of MβCD and metabolic stress on the distribution of GLUT1 between different membrane domains in Clone 9 cells

The effects of cholesterol depletion on glucose uptake by Clone 9 cells suggested that GLUT1 might be associated with cholesterol-rich regions of the membrane. Membrane domains that are highly enriched in cholesterol and glycolipids can be isolated on the basis of their insolubility in some non-ionic detergents at 4 °C. Because of their low buoyant density, the detergent-insoluble microdomains or 'lipid rafts' float up to the lower density regions when centrifuged on appropriate density gradients, whereas detergent-solubilized membrane proteins are recovered from the denser portions of the gradients. To investigate the possible association of GLUT1 with cholesterol-rich membrane domains in the present study, cells were treated with Triton X-100 and then soluble and insoluble proteins were separated by centrifugation on a Nycodenz linear step gradient. Equal aliquots from each of the 12 fractions collected from the gradients were analysed by SDS/PAGE followed by Western blotting. Figure 4(A) is representative of a typical analysis: the GLUT1 protein was present not only in the high-density region of the gradient (fractions 8 and 9) but also in the low-density region (fractions 4 and 5) characteristically occupied by detergent-insoluble membrane domains. Densitometric analyses of the blots showed that 36 ± 0.5 % ($n = 4$) of the total GLUT1 protein was located in the low-density region of the gradient: interestingly, other workers have reported that approx. 37 % of the homologous transporter GLUT4 present in detergent-solubilized plasma membranes from 3T3-L1 adipocytes is similarly associated with lipid-raft fractions on density gradients [33]. The level of GLUT1 estimated by densiotometric analysis in fractions 4 and 5 was 13 ± 3 ($n = 3$)-fold greater in untreated cells (Figure 4A) compared with cholesterol-depleted cells (Figure 4B) and 3 ± 0.5 ($n = 3$)-fold greater in untreated cells compared with cells stressed by exposure to sodium azide (Figure 4C).

Co-distribution of the GLUT1 protein with other lipid-raft proteins

The migration of a substantial proportion of GLUT1 to the low density region of Nycodenz gradients during fractionation of Clone 9 cell detergent lysates suggested that the transporter might in part be associated with lipid rafts. To probe this hypothesis further, we next examined the co-distribution of the transporter with lipid-raft marker proteins, using sucrose-density-gradient centrifugation of detergent lysates. The proteins stomatin (31 kDa) and the caveolin (22 kDa) are known to be associated with lipid rafts in a variety of cells and so were used as markers for these structures [34–36]. Proteins present in each fraction from the density gradients were separated by SDS/PAGE, transferred to nitrocellulose membranes and then immunoblotted. While the bulk of the Clone 9 cell protein was found in the high-density region at the bottom of the sucrose gradient (Figure 5A), a substantial proportion (45 ± 7 %) of the total GLUT1 was present at the boundary between the 5 % and 35 % sucrose layers (Figure 5B). A similarly high proportion of the total cellular content of both stomatin and caveolin was also present in this region of the gradient, confirming that it contained lipid rafts (Figure 5B). In contrast, the water-soluble protein tubulin and the transferrin receptor, a membrane protein known not to partition with lipid rafts [33], were confined to the high-density region of the gradient,

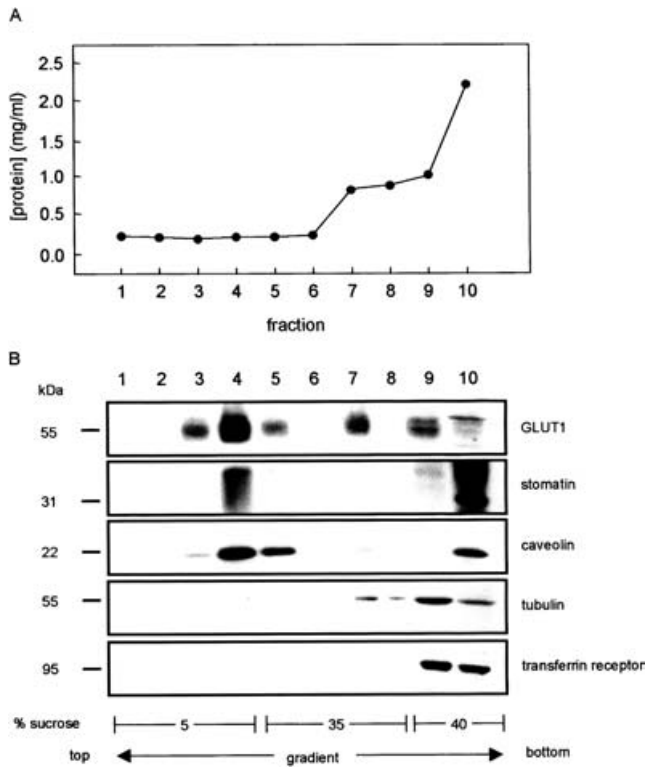

Figure 5 Co-localization of GLUT1 and lipid-raft proteins in Clone 9 cells

Confluent Clone 9 cells were washed in KRH/EDTA, scraped into a Falcon tube, precipitated by centrifugation and solubilized in 0.5 ml of 0.5 % Triton X-100 in KRH/EDTA buffer at 4 °C. Nuclei and cell debris were removed by low-speed centrifugation and the resultant supernatant was separated on a sucrose gradient by ultracentrifugation as described in detail in the Materials and methods section. (**A**) Typical profile of protein concentrations (means from two independent determinations) in gradient fractions after centrifugation. (**B**) Western blots of 25 μl protein samples from the gradient fractions: proteins were separated by electrophoresis on an SDS/10 % (w/v) polyacrylamide gel, transferred to nitrocellulose membranes and stained with antibodies against the proteins indicated.

confirming the solubilization by detergent of non-raft regions of the cell membranes (Figure 5B).

Effects of cholesterol depletion and metabolic stress on the spatial distribution of GLUT1 in Clone 9 cell plasma membranes

The co-localization of a proportion of GLUT1 with caveolin and stomatin during density-gradient fractionation of detergent-solubilized Clone 9 cells strongly suggested that the transporter was located, at least in part, in cholesterol-rich subdomains of the plasma membrane. However, it remains unclear whether such detergent-insoluble fractions of membranes reflect solely the properties of pre-existing domains, or are in part generated by the action of the detergent itself [37]. To provide independent information about the localization of GLUT1 prior to detergent treatment of the cells, immunocytochemistry of plasma membrane lawns was therefore used to assess the lateral distribution of the transporters. As illustrated in Figure 6, GLUT1 exhibited a markedly punctate staining pattern in membranes prepared from untreated cells, indicating the presence of 'microdomains' enriched in the transporters rather than an even distribution over the membrane surface. The microdomains were of variable morphology and size, but typically exhibited diameters of up to approx. 1 μm, similar to the dimensions reported for some types of lipid raft. No co-localization was observed when membranes were simultaneously stained with antibodies against GLUT1 and clathrin, indicating that the transporter-enriched domains did not correspond to coated pits (results not shown).

Cholesterol depletion had a marked effect both on the size of the plasma membrane sheets produced from MβCD-treated cells and upon the distribution of GLUT1 observed in them. The mean cell diameter decreased almost 2-fold after 1 h of treatment (Figure 6): a similar decrease in cell size has also been noted in plasma membrane lawns prepared from 3T3-L1 adipocytes that have been treated with 10 mM MβCD [38]. In parallel, the number of GLUT1-enriched microdomains per unit area of membrane decreased by 73 ± 4 % ($n = 3$), apparently because of selective loss of the smaller microdomains (Figure 6, bottom panels). While treatment of cholesterol-replete cells with sodium azide had little effect on the size of the plasma membrane sheets, it also led to a significant decrease (30 ± 1 %; $n = 3$) in the number of GLUT1 microdomains per unit area (Figure 6). The same effect was observed when either an antibody raised against the central cytoplasmic loop of GLUT1 (residues 231–246; results not shown) or antibody raised against the C-terminus of the transporter (residues 477–492; Figure 6) was employed as the primary antibody. It was of course not possible to equate these punctate staining areas directly with the detergent-insoluble membrane domains identified by density-gradient centrifugation. Similarly, double-labelling experiments revealed only partial co-localization of GLUT1 and caveolin, suggesting that the GLUT1 microdomains did not correspond primarily to caveolae (results not shown). However, the decreased number of these stained regions in cholesterol-depleted and azide-treated cells was consistent with the relocation of a proportion of the plasma membrane GLUT1 molecules into the bulk of the membrane, where they might have encountered a different lipid environment.

Association of GLUT1 with stomatin

The molecular mechanisms involved in the clustering of GLUT1 molecules in microdomains of the plasma membrane, identified either by their detergent insolubility or appearance on immunostained plasma membrane lawns, are unknown. However, it has recently been suggested that the 31 kDa lipid-raft protein, stomatin, associates with GLUT1 and that this interaction may play a role in GLUT1 function [20,39]. These conclusions were reached as a result of the observation that a proportion of stomatin and GLUT1 could be co-immunoprecipitated from detergent lysates of red blood cell membranes and Clone 9 cells, and that over-expression of stomatin in the latter cell type depressed the basal rate of GLUT1 glucose-transport activity. To investigate the possibility that stomatin was involved in GLUT1 clustering, in the present study the spatial relationships between the two types of protein were examined by immunostaining plasma membrane lawns concomitantly for GLUT1 and stomatin (Figure 7). Like GLUT1, stomatin was found to exhibit a punctate distribution. However, only a small minority of the GLUT1 and stomatin staining was co-localized, suggesting that the localization of GLUT1 in microdomains did not depend on an association with stomatin.

The small extent of co-localization of GLUT1 and stomatin might have reflected the relatively low abundance of the latter in Clone 9 cells [20]. However, some interaction between the two proteins was suggested by the observation that over-expression of stomatin in Clone 9 cells reduced glucose-transport activity [20]. To examine further the possible association of GLUT1 and stomatin, and the regions of the two proteins that might be involved in this interaction, unfixed plasma membrane lawns prepared from Clone 9 cells were therefore incubated with or

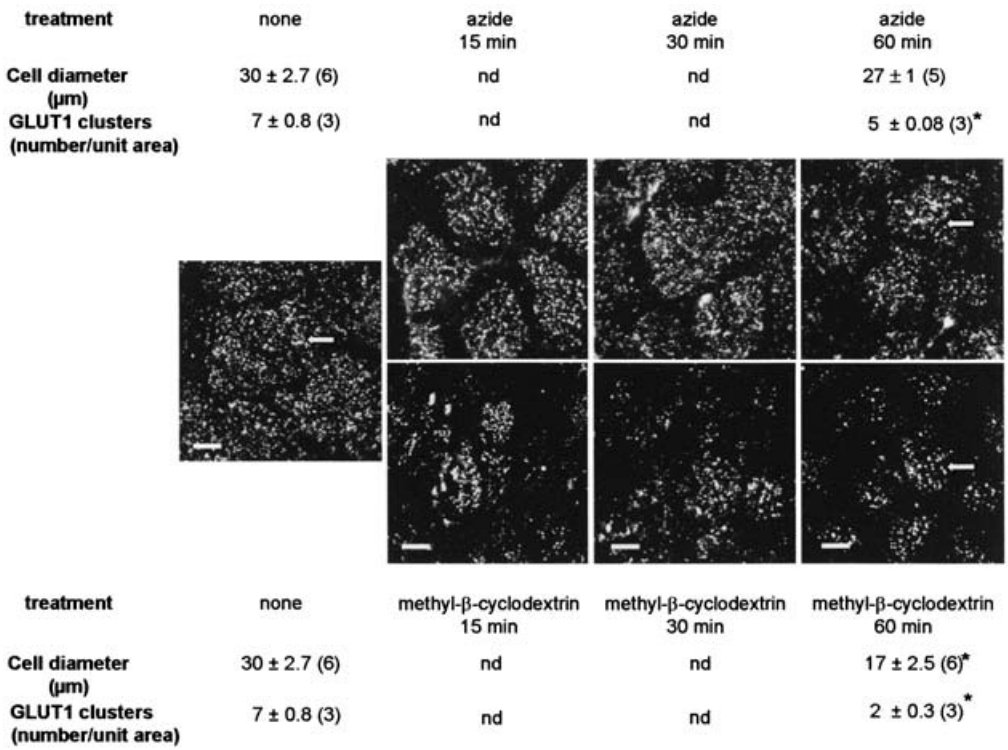

Figure 6 Effects of cholesterol depletion and metabolic stress on the spatial distribution of GLUT1 in Clone 9 cell plasma membranes

Cells were exposed to 10 mM MβCD or 5 mM sodium azide for the times indicated. Plasma membrane sheets were then prepared, immunostained with polyclonal antibodies against the C-terminal region (residues 477–492) of GLUT1 and visualized as described in the Materials and methods section. Cell diameter data (mean $\pm$ S.D.) were pooled from two experiments in which five or six fields (*n*) were measured, each containing an average of eight cells. The arrows indicate the clusters of GLUT1 transporters. The number of GLUT1 microdomains were estimated (mean $\pm$ S.E.M) from three independent experiments (*n*), in each of which the number of punctate regions stained with the antibodies in three regions of interest were counted in an average of ten cells. *Significantly different ($P < 0.05$) from control (untreated cells). Scale bars, 10 μm; nd, not determined.

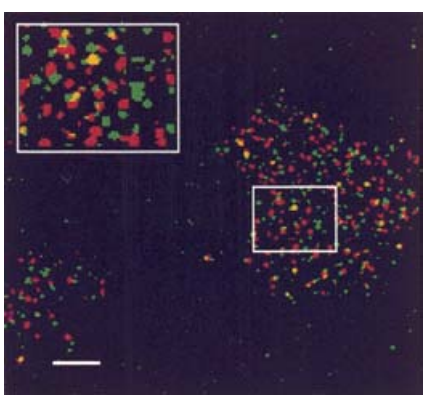

Figure 7 Relative distributions of GLUT1 and stomatin in plasma membranes

Clone 9 cell plasma membrane lawns were simultaneously stained with rabbit antibodies against the central cytoplasmic loop of GLUT1 and sheep antibodies against stomatin as described in the Materials and methods section. Bound antibodies were detected using Texas Red and Alexa Fluor488 (green) conjugates respectively, and visualized by deconvolution fluorescence microscopy. The inset shows a 2-fold magnified image. Scale bar, 10 μm.

without the purified C-terminal hydrophilic domain of stomatin before immunostaining for GLUT1. When the antibody raised against the central cytoplasmic loop of GLUT1 (residues 231–246) was employed for this purpose, identical staining patterns were seen for samples treated with or without the stomatin domain (Figure 8). However, staining with an antibody raised against the C-terminus of the transporter (residues 477–492) was reduced more than 5-fold by pre-incubation of the membranes with the stomatin fragment. This finding suggests that the C-terminal epitope of GLUT1 was selectively masked by interaction with the hydrophilic domain of stomatin. Interestingly in basal conditions a smaller number of clusters were apparently stained by antibodies against the C-terminal region than by antibodies against the central loop region of GLUT1. This observation is also indicative of masking of the GLUT1 C-terminus in basal conditions that prevents universal access of the C-terminal antibody to all GLUT1 present in the plasma membrane.

DISCUSSION

As described in the Introduction, the transport activity of the reconstituted GLUT1 protein is very sensitive to its phospholipid and cholesterol environment [6]. Changes in the cholesterol content of the cell membrane might therefore be expected to affect the activity of the transporter. In the present study we demonstrated that cholesterol depletion of Clone 9 cells by treatment with MβCD caused a significant increase in the V_{max} for transport with little effect on K_m. Interestingly, these changes in transport kinetics mimicked those seen in cells subjected to osmotic or metabolic stress [2,22,40]. Moreover, no additional increase in transport activity was found when cholesterol depleted cells were subjected to metabolic stress by treatment with sodium azide. It was therefore possible that the two stimuli for transport activation involved the same pool of transporters and activation mechanism(s). Recently AMPK, a key sensor of cellular energy

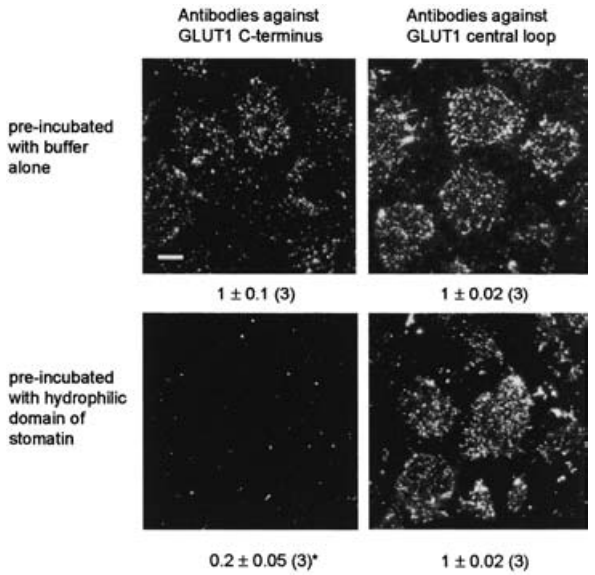

Figure 8 Masking of GLUT1 C-terminal epitopes by association with stomatin

Clone 9 cell plasma membrane lawns were treated with buffer alone (control, top panels) or with the C-terminal domain of stomatin (bottom panels) as detailed in the Materials and methods section. They were then stained with antibodies either against the central cytoplasmic loop of GLUT1 (right-hand panels) or against the GLUT1 C-terminal region (left-hand panels) as described in the Materials and methods section. Images are representative of three separate experiments. Image intensities (mean ± S.E.M.; $n = 3$) relative to buffer-treated samples are shown below each panel, and were obtained using NIH Image J software. *Significant reduction in staining intensity ($P < 0.01$) in comparison with control (untreated cells). Scale bar, 10 μm.

status, was shown to play a role in the signal transduction pathway leading to stimulation of glucose uptake in Clone 9 cells subjected to stress [3,41]. However, because no dramatic decrease in ATP levels or increase in phosphorylation levels of AMPK were evident in cholesterol-depleted cells, the increase in transporter activity measured in these cells was unlikely to have involved activation of the AMPK pathway. Previous reports from this laboratory have demonstrated the involvement of the stress-activated kinases p38 MAPK and JNK in stress-stimulated transporter activity [2,22]. However, the lack of effect of MβCD treatment on the phosphorylation state of these kinases in Clone 9 cells, seen in the present study, indicates that they are not involved in the mechanism leading to increased transporter activity in cholesterol-depleted cells.

Instead, a possible explanation for the stimulation of hexose uptake was that GLUT1 activation was triggered by a change in its lipid environment as a result of cholesterol depletion of lipid microdomains (lipid rafts) in the plasma membrane. Traditionally, lipid rafts have been isolated at 4 °C using non-ionic detergents and density-gradient ultracentrifugation [7,42,43]. Here we used such methods to show that a substantial proportion of Clone 9 cell GLUT1 molecules co-migrated to the low-density region of gradients together with the lipid-raft proteins caveolin and stomatin. Its redistribution to higher-density, detergent-soluble fractions after depletion of cell cholesterol suggested that, like GLUT4 in adipocytes [33] and GLUT1 in HeLa-derived hybrid CGL4 cells [19], GLUT1 in Clone 9 cells was located in cholesterol-rich lipid microdomains of the plasma membrane. In parallel experiments, as also reported by other authors [44], when cells were metabolically stressed with sodium azide, GLUT1 showed a similar but less marked migration from lipid rafts.

Although evidence for the clustering of GLUT1 in microdomains of the Clone 9 cell plasma membrane was also obtained by immunocytochemistry, co-localization experiments with caveolin showed these microdomains did not correspond to caveolae. Similar findings have been reported for GLUT4: electron microscopic studies of white adipose cells showed that only about 2% of the transporter was located in caveolae despite the fact that these comprise about 17% of the cell surface [45]. Moreover, cholesterol depletion, which is known to cause disruption of caveolae in other cell types [17,46] and had the same effect on Clone 9 cells (present study, results not shown), did not completely disperse plasma membrane clusters of GLUT1 in Clone 9 cells. Interestingly however, the abundance of GLUT1 clusters in the plasma membrane was reduced both in cells treated with MβCD and in those exposed to metabolic stress, consistent with relocation of a proportion of the transporters from the putative cholesterol-rich lipid microdomains to the surrounding membrane. The proposed interaction of the C-terminal epitope of GLUT1 and the hydrophilic domain of stomatin is supported by previous reports of association *in vitro* between full-length stomatin and a GST fusion protein bearing the C-terminal region of GLUT1 [20,39]. The ability of antibodies against the C-terminal region of GLUT1 efficiently to stain the transporter in untreated membranes may reflect the low natural abundance of endogenous stomatin in Clone 9 cells: excess stomatin may be necessary to saturate completely all the C-terminal binding sites of GLUT1.

While direct evidence has been obtained that stimulation of hexose transport by stress involves the 'unmasking' of cryptic permeant-binding sites in GLUT1, the precise mechanism of this process remains unclear [3]. However, the redistribution of GLUT1 from cholesterol-rich microdomains of the plasma membrane reported here and elsewhere [44], together with the known sensitivity of GLUT1 to its lipid environment [6], suggest a possible role for lipid rafts in the stress-induced activation of the transporter in Clone 9 cells. Whether transporter redistribution involves altered interactions with lipid-raft protein components remains unclear. However, the partial co-localization of GLUT1 and stomatin reported here, together with the observed masking of the GLUT1 C-terminus by the cytoplasmic domain of this raft protein and functional studies reported elsewhere [20,39], indicate that further detailed examination of such protein–protein interactions is warranted.

This work was supported by grants from the BBSRC Bioimaging Initiative, the MRC and the Wellcome Trust (to S.A.B.), and by the Sir Jules Thorn Trust (to G.W.S.). We thank Margaret Chetty for technical assistance.

REFERENCES

1 Mercado, C. L., Loeb, J. N. and Ismail-Beigi, F. (1989) Enhanced glucose transport in response to inhibition of respiration in Clone 9 cells. Am. J. Physiol. **257**, C19–C28
2 Barros, L. F., Barnes, K., Ingram, J. C., Castro, J., Porras, O. H. and Baldwin, S. A. (2001) Hyperosmotic shock induces both activation and translocation of glucose transporters in mammalian cells. Eur. J. Physiol. **442**, 614–621
3 Barnes, K., Ingram, J. C., Porras, O. H., Barros, L. F., Hudson, E. R., Fryer, L. G. D., Foufelle, F., Carling, D., Hardie, D. G. and Baldwin, S. A. (2002) Activation of GLUT1 by metabolic and osmotic stress: potential involvement of AMP-activated protein kinase (AMPK). J. Cell Sci. **115**, 2433–2442
4 Shetty, M., Loeb, J. N., Vikstrom, K. and Ismailbeigi, F. (1993) Rapid activation of GLUT-1 glucose transporter following inhibition of oxidative phosphorylation in clone-9 cells. J. Biol. Chem. **268**, 17225–17232
5 Hamrahian, A. H., Zhang, J. Z., Elkhairi, F. S., Prasad, R. and Ismailbeigi, F. (1999) Activation of Glut1 glucose transporter in response to inhibition of oxidative phosphorylation – role of sites of mitochondrial inhibition and mechanism of Glut1 activation. Arch. Biochem. Biophys. **368**, 375–379

6 Carruthers, A. and Melchior, D. L. (1984) Human erythrocyte hexose transporter activity is governed by bilayer lipid composition in reconstituted vesicles. Biochemistry **23**, 6901–6911
7 Simons, K. and Ikonen, E. (1997) Functional rafts in cell membranes. Nature (London) **387**, 569–572
8 Pralle, A., Keller, P., Florin, E. L., Simons, K. and Horber, J. K. (2000) Sphingolipid-cholesterol rafts diffuse as small entities in the plasma membrane of mammalian cells. J. Cell Biol. **148**, 997–1008
9 Schutz, G. J., Kada, G., Pastushenko, V. P. and Schindler, H. (2000) Properties of lipid microdomains in a muscle cell membrane visualized by single molecule microscopy. EMBO J. **19**, 892–901
10 Edidin, M. (2001) Shrinking patches and slippery rafts: scales of domains in the plasma membrane. Trends Cell Biol. **11**, 492–496
11 Varma, R. and Mayor, S. (1998) GPI-anchored proteins are organized in submicron domains at the cell surface. Nature (London) **394**, 798–801
12 Hooper, N. M. (1999) Detergent-insoluble glycosphingolipid/cholesterol-rich membrane domains, lipid rafts and caveolae (review). Mol. Membrane Biol. **16**, 145–156
13 Smart, E. J. and Anderson, R. G. (2002) Alterations in membrane cholesterol that affect structure and function of caveolae. Methods Enzymol. **353**, 131–139
14 Simons, K. and Toomre, D. (2000) Lipid rafts and signal transduction. Nat. Rev. Mol. Cell Biol. **1**, 31–39
15 Baumann, C. A., Ribon, V., Kanzaki, M., Thurmond, D. C., Mora, S., Shigematsu, S., Bickel, P. E., Pessin, J. E. and Saltiel, A. R. (2000) CAP defines a second signalling pathway required for insulin-stimulated glucose transport. Nature (London) **407**, 202–207
16 Chiang, S. H., Baumann, C. A., Kanzaki, M., Thurmond, D. C., Watson, R. T., Neudauer, C. L., Macara, I. G., Pessin, J. E. and Saltiel, A. R. (2001) Insulin-stimulated GLUT4 translocation requires the CAP-dependent activation of TC10. Nature (London) **410**, 944–948
17 Watson, R. T., Shigematsu, S., Chiang, S. H., Mora, S., Kanzaki, M., Macara, I. G., Saltiel, A. R. and Pessin, J. E. (2001) Lipid raft microdomain compartmentalization of TC10 is required for insulin signaling and GLUT4 translocation. J. Cell Biol. **154**, 829–840
18 Watson, R. T., Furakawa, M., Chiang, S. H., Boeglin, D., Saltiel, A. R. and Pessin, J. E. (2002) The CAAX targeting motif of TC10 directs its intracellular trafficking, lipid raft microdomain localization, and its ability to modulate insulin-stimulated GLUT4 translocation. Diabetes **51**, A296
19 Sakyo, T. and Kitagawa, T. (2002) Differential localization of glucose transporter isoforms in non-polarized mammalian cells: distribution of GLUT1 but not GLUT3 to detergent-resistant membrane domains. Biochim. Biophys. Acta **1567**, 165–175
20 Zhang, J. Z., Abbud, W., Prohaska, R. and Ismail-Beigi, F. (2001) Overexpression of stomatin depresses GLUT-1 glucose transporter activity. Am. J. Physiol. **280**, C1277–C1283
21 Lennon, G. G., Auffray, C., Polymeropoulos, M. and Soares, M. B. (1996) The I.M.A.G.E. Consortium: an integrated molecular analysis of genomes and their expression. Genomics **33**, 151–152
22 Barros, L. F., Marchant, R. B. and Baldwin, S. A. (1995) Dissection of stress-activated glucose transport from insulin-induced glucose transport in mammalian cells using wortmannin and ML-9. Biochem. J. **309**, 731–736
23 Fukasawa, M., Nishijima, M., Itabe, H., Takano, T. and Hanada, K. (2000) Reduction of sphingomyelin level without accumulation of ceramide in Chinese hamster ovary cells affects detergent-resistant membrane domains and enhances cellular cholesterol efflux to methyl-beta-cyclodextrin. J. Biol. Chem. **275**, 34028–34034
24 Naslavsky, N., Stein, R., Yanai, A., Friedlander, G. and Taraboulos, A. (1997) Characterization of detergent-insoluble complexes containing the cellular prion protein and its scrapie isoform. J. Biol. Chem. **272**, 6324–6331
25 Dermine, J. F., Duclos, S., Garin, J., St Louis, F., Rea, S., Parton, R. G. and Desjardins, M. (2001) Flotillin-1-enriched lipid raft domains accumulate on maturing phagosomes. J. Biol. Chem. **276**, 18507–18512
26 Davies, A., Ciardelli, T. L., Lienhard, G. E., Boyle, J. M., Whetton, A. D. and Baldwin, S. A. (1990) Site-specific antibodies as probes of the topology and function of the human erythrocyte glucose transporter. Biochem. J. **266**, 799–808
27 Coles, S. E., Ho, M. M., Chetty, M. C., Nicolaou, A. and Stewart, G. W. (1999) A variant of hereditary stomatocytosis with marked pseudohyperkalaemia. Br. J. Haematol. **104**, 275–283
28 Smith, P. K., Krohn, R. I., Hermanson, G. T., Mallia, A. K., Gartner, F. H., Provenzano, M. D., Fujimoto, E. K., Goeke, N. M., Olson, B. J. and Klenk, D. C. (1985) Measurement of protein using bicinchoninic acid. Anal. Biochem. **150**, 76–85
29 Carruthers, A. and Melchior, D. L. (1988) Effects of lipid environment on membrane transport: The human erythrocyte sugar transport protein/lipid bilayer system. Annu. Rev. Physiol. **50**, 257–271
30 Christian, A. E., Haynes, M. P., Phillips, M. C. and Rothblat, G. H. (1997) Use of cyclodextrins for manipulating cellular cholesterol content. J. Lipid Res. **38**, 2264–2272
31 Shetty, M., Loeb, J. N. and Ismail-Beigi, F. (1992) Enhancement of glucose transport in response to inhibition of oxidative metabolism: pre- and posttranslational mechanisms. Am. J. Physiol. **262**, C527–C532
32 Cano, E., Hazzalin, C. A. and Mahadevan, L. C. (1994) Anisomycin-activated protein kinases p45 and p55 but not mitogen-activated protein kinases ERK-1 and -2 are implicted in the induction of c-*fos* and c-*jun*. Mol. Cell. Biol. **14**, 7352–7362
33 Chamberlain, L. H. and Gould, G. W. (2002) The vesicle- and target-SNARE proteins that mediate Glut4 vesicle fusion are localized in detergent-insoluble lipid rafts present on distinct intracellular membranes. J. Biol. Chem. **277**, 49750–49754
34 Salzer, U. and Prohaska, R. (2001) Stomatin, flotillin-1, and flotillin-2 are major integral proteins of erythrocyte lipid rafts. Blood **97**, 1141–1143
35 Mairhofer, M., Steiner, M., Mosgoeller, W., Prohaska, R. and Salzer, U. (2002) Stomatin is a major lipid-raft component of platelet alpha granules. Blood **100**, 897–904
36 Galbiati, F., Razani, B. and Lisanti, M. P. (2001) Emerging themes in lipid rafts and caveolae. Cell **106**, 403–411
37 Edidin, M. (2003) The state of lipid rafts: from model membranes to cells. Annu. Rev. Biophys. Biomol. Struct. **32**, 257–283
38 Weeks, L. K., Liu, P., Leffler, B. J. and Elmendorf, J. S. (2002) Physical changes in cholesterol/sphingomyelin-rich membrane rafts augment plasma membrane GLUT4 content. Diabetes **51** (suppl. 2), A325
39 Zhang, J. Z., Hayashi, H., Ebina, Y., Prohaska, R. and Ismailbeigi, F. (1999) Association of stomatin (Band 7.2b) with Glut1 glucose transporter. Arch. Biochem. Biophys. **372**, 173–178
40 Shi, Y. W., Liu, H. Z., Vanderburg, G., Samuel, S. J., Ismailbeigi, F. and Jung, C. Y. (1995) Modulation of GLUT1 intrinsic activity in clone 9 cells by inhibition of oxidative phosphorylation. J. Biol. Chem. **270**, 21772–21778
41 Abbud, W., Habinowski, S., Zhang, J. Z., Kendrew, J., Elkairi, F. S., Kemp, B. E., Witters, L. A. and Ismail-Beigi, F. (2000) Stimulation of AMP-activated protein kinase (AMPK) is associated with enhancement of Glut1-mediated glucose transport. Arch. Biochem. Biophys. **380**, 347–352
42 London, E. (2002) Insights into lipid raft structure and formation from experiments in model membranes. Curr. Opin. Struct. Biol. **12**, 480–486
43 Brown, D. A. and London, E. (1997) Structure of detergent-resistant membrane domains: does phase separation occur in biological membranes? Biochem. Biophys. Res. Commun. **240**, 1–7
44 Rubin, D. and Ismail-Beigi, F. (2003) Distribution of Glut1 in detergent-resistant membranes (DRMs) and non-DRM domains: effect of treatment with azide. Am. J. Physiol. Cell Physiol. **285**, C377–C383
45 Malide, D., Ramm, G., Cushman, S. W. and Slot, J. W. (2000) Immunoelectron microscopic evidence that GLUT4 translocation explains the stimulation of glucose transport in isolated rat white adipose cells. J. Cell Sci. **113**, 4203–4210
46 Parpal, S., Karlsson, M., Thorn, H. and Stralfors, P. (2001) Cholesterol depletion disrupts caveolae and insulin receptor signaling for metabolic control via insulin receptor substrate-1, but not for mitogen-activated protein kinase control. J. Biol. Chem. **276**, 9670–9678

Received 5 August 2003/28 October 2003; accepted 14 November 2003
Published as BJ Immediate Publication 14 November 2003, DOI 10.1042/BJ20031186